

Synthesis and characterization of peptide nanostructures chemisorbed on gold†

Joëlle Martin Boutin, Julie Richer, Mélanie Tremblay, Véronique Bissonette and Normand Voyer*

Received (in Durham, UK) 7th December 2006, Accepted 5th February 2007

First published as an Advance Article on the web 7th March 2007

DOI: 10.1039/b617877d

We report the synthesis and the use of a peptide nanostructure for the preparation of modified gold nanoparticles and gold surfaces. A helical peptide bearing six crown ether side chains, known to form an artificial ion channel, was modified at its termini with biotin and a disulfide group. Using this peptide nanostructure, we were able to prepare gold nanoparticles and self-assembled monolayers on gold surfaces. FTIR and IRRAS experiments demonstrated that the peptide nanostructures retained their helical conformation when chemisorbed on a gold surface and that they are oriented with tilt angles around 55° from the surface normal. AFM studies confirmed that the peptide nanostructures formed well defined and regular surfaces with clusters having average heights of 5–6 nm, in close agreement with the size of the nanostructure.

Introduction

Since the first description of biosensors by Schultz, many affinity-based natural or artificial molecular detection systems have been reported.¹ Recent reports described sensors with improved sensitivity for detection and quantification of specific analytes both *in vivo* and *in vitro*. Testing of drugs, medical diagnosis, and environmental and clinical monitoring constitute only a few of the applications for biosensors, an area of great interest.^{2–4}

Metallic surfaces, such as those of gold, and especially gold nanoparticles, are often used in detection devices. These materials are useful in providing a metallic central core whose physical and electronic properties as well as chemical nature can be controlled.^{3,5,6} The most intensely studied nanosized metallic system is the thiolate-protected gold nanoparticles first reported by Brust and Schiffrin in 1994.⁷ Their self-assembled nature makes them easy to synthesize.⁸ Due to the thiol functionality, they are highly stable both in solution and in the solid state. This characteristic makes them extremely interesting for nanometer-size functional systems. They are employed in many applications, especially in electronics, optics, genomics, proteomics, biomedical and bioanalytical areas.⁶

Along the same lines, the chemisorption of thiols on an evaporated gold film allows the spontaneous formation of a self-assembled monolayer (SAM) on a zerovalent gold substrate. The high stability of thiol SAMs formed on gold substrates and their resistance to atmospheric contamination also make gold surfaces a choice support for the development of analytical and biological tools.⁹

We have recently reported the design and use of nanoscale peptide structures that bear a biological recognition element and act as artificial channels.¹⁰ Our results demonstrate the usefulness of crown ether peptide nanostructures as “molecular transducers” in the development of rapid fluorescent detection assays to biologically monitor relevant analytes. To develop more practical sensors, we sought to prepare functionalized gold nanoparticles and surfaces using these nanostructures. Here, we present the design and synthesis of such supramolecular systems.

Design

Our working hypothesis is based on the premise that gold nanoparticle properties would be more sensitive to the presence of biological molecules of interest when modified with an artificial ion channel (Fig. 1).^{11,12} The molecular system at the basis of the present study, **1**, was built from a helical peptide bearing six crown ethers aligned to form a synthetic ion channel. It was modified at the *N*-terminal with biotin to serve as a recognition element. The well-known biotin–avidin model

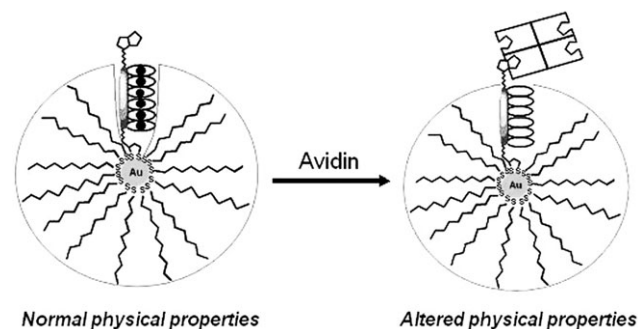
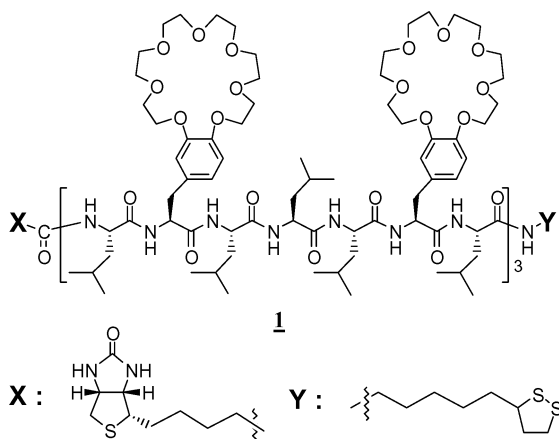


Fig. 1 Working hypothesis: the complexation of a biological analyte (in this case avidin) to the recognition element (here biotin) coupled to the molecular transducer lead to significant changes in gold properties.

Centre de recherche sur la fonction, la structure, et l'ingénierie des protéines, Département de chimie, Faculté des Sciences et de Génie, Université Laval, Québec, Canada G1K 7P4

† Dedicated to Professor George Gokel on the occasion of his 60th birthday.

system was chosen to demonstrate the proof-of-concept of this strategy. This system has been widely used in model studies due to its strong and stable complexation and high specificity.^{13,14} As for the anchoring group, a disulfide derived from lipoic acid was added to the C terminal of the peptide to allow a strong chemisorption on gold nanoparticles or surfaces. The disulfide function of lipoic acid has already been reported to readily anchor polypeptides on gold.^{15,16}



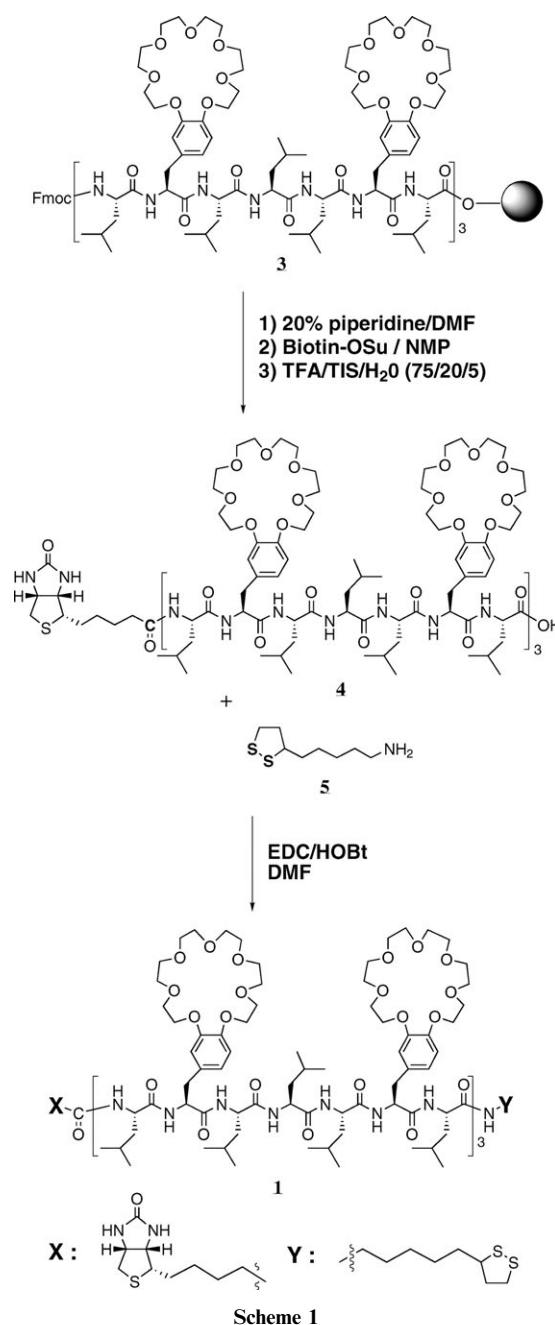
Results and discussion

Synthesis

The synthesis of target peptide nanostructure **1** is shown in Scheme 1. Synthesis of **3** was done on Wang resin using Fmoc procedures. The required Fmoc-crown ether (CE) amino acid was synthesized by deprotection of the Boc protected analog using 4 M HCl in dioxane, followed by re-protection with Fmoc-OSu in a mixture of acetonitrile and water. The synthesis of Boc-CE amino acid was reported previously.¹² Incorporation of biotin at the N-terminal position was directly performed on solid support, as shown in Scheme 1. After deprotection of the Fmoc group with piperidine, the N-terminal amino group was coupled to biotin, previously activated with N-hydroxysuccinimide (Biotin-OSu).¹⁴ Finally, cleavage of the resin, in acidic conditions, provided the corresponding biotinylated peptide **4**.

Incorporation of the disulfide function at the C-terminal position of peptides was accomplished by coupling lipoamine **5** in solution to the cleaved peptide **4**. Lipoamine **5** was obtained by the reduction of commercial 6-thioctic amide, followed by air oxidation to regenerate disulfide, according to the procedure described by Morita *et al.*¹⁷ Peptide **4** was activated with EDC/HOBt in DMF and then coupled to lipoamine at room temperature for 24 h.¹⁸ Purification of crude product was done by gel filtration on Sephadex LH-20 using methanol as eluant to provide the desired peptide **1**, which was characterized by MS. RP-HPLC analysis demonstrated a purity >90% and less than 5% of epimerization (Fig. 2).

CD studies of peptide **1** in TFE confirmed that the peptide framework prefers to adopt a strong α -helical conformation. The mean residue molar ellipticity of **1** ($[\theta]_{222} = -3.5 \times 10^5$)



Scheme 1

compares well with the one of the analog peptide nanostructure without terminal groups **2** ($[\theta]_{222} = -3.2 \times 10^5$).

Gold nanoparticles

To synthesize gold nanoparticles modified with **1**, we tried two different strategies. We first tried a displacement reaction¹⁹ on nanoparticles prepared using three alkane thiols (C_{18} -SH, C_{10} -SH and C_4 -SH). The exchange of these thiols by peptide **1** (ratio of gold nanoparticle : peptide of 10 : 1 or 2 : 1) did not proceed to a significant extent. Peptide **1** could not be detected by NMR or IR of the gold nanoparticles recovered after the exchange processes. Consequently, we prepared the modified nanoparticles using a mixture of **1** and a C_{18} thiol during

synthesis. The reduction of the metal salt with NaBH_4 under these conditions gave the desired functionalized gold nanoparticles (Scheme 2). Nanoparticles with pure alkane thiol were also prepared for controls.

Characterization of gold nanoparticles

Functionalized gold nanoparticles were first characterized using ATR (attenuated total reflection) spectroscopy. ATR results are shown in Fig. 3. The presence of the amide I and II bands on ATR spectra of the gold nanoparticles formed with peptide **1** clearly demonstrates the chemisorption of peptides on the particles. The amide I and amide II band at 1656 and 1545 cm^{-1} , respectively, indicate retention of the α -helix conformation of the peptidic nanostructure after chemisorption on gold nanoparticles.²⁰ Attempts to determine the ratio of peptide to lipid on gold nanoparticles by NMR failed due to heavy broadening of signals.

The sizes and shape of nanoparticles were analyzed using transmission electron microscopy (TEM). Representative images obtained are shown in Fig. 4. Nanoparticle diameters vary between 2 and 5 nm. The average size of nanoparticles functionalized with peptide and thiol was a little smaller than the average size of nanoparticles prepared with alkanethiol only. Generally, the shape of particles was more uniform when a mixture of thiol and peptide was used (Fig. 4, left). It is important to note that the addition of peptide in the preparation of nanoparticles does not induce aggregation. Hence, these results demonstrate the feasibility of preparing gold nanoparticles bearing a functionalized peptide structure. Since it is reasonable to believe that the reporter group on the *N*-terminal is sticking out of the hydrophobic shell, these nanoparticles could be used for capturing a biological receptor, in this case avidin.

Peptide nanostructure modified gold surfaces

We also prepared gold surfaces modified with pure peptide nanostructure **1**. After the usual cleaning procedures, chemisorption reactions on gold surfaces were performed by immersion in a solution of pure functionalized peptide **1** in TFE. The choice of TFE was based on previous studies that demonstrated that **1** and the nanostructures of analogous peptides adopt a strong helical conformation and are unaggregated in that solvent. Following incubation, samples were rinsed several times with TFE to eliminate free peptides and other contaminants. Samples were then dried under a stream of nitrogen prior to analysis.

Characterization of peptide monolayers

Fourier transform infrared reflection-absorption spectroscopy (IRRAS) is a useful technique to study monolayer and sub-monolayer amounts of adsorbates on metal surfaces.²¹ The IRRAS spectrum of peptide **1** SAM on gold is shown in Fig. 5. Results clearly demonstrate the presence of the peptide nano-

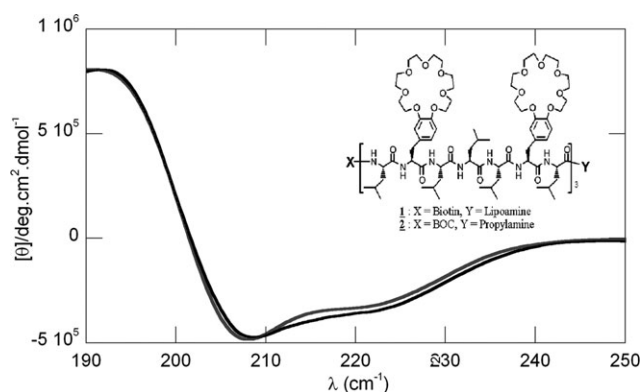


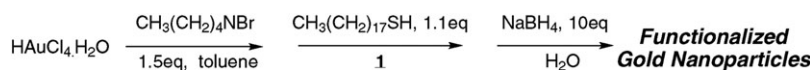
Fig. 2 Circular dichroism spectra of peptide nanostructure **1** (grey line) and control nanostructure **2** (black line).

structure on the metallic surface as indicated by the presence of amide I and II bands in the spectrum. The strong amide I band at 1657 cm^{-1} demonstrated that **1** still preserved its strong helical conformation when chemisorbed on gold.²⁰ Hence, it can be assumed reasonably that the crown ether side chains are aligned on top of each other.

On the basis of the absorbance intensity ratio of amide I/amide II bands in the IRRAS spectra, we calculated the tilt angle of the helix axis from the surface normal. Indeed, the molecular orientation of helical structures on gold surfaces can be calculated using eqn (1), assuming a uniform distribution of the helical peptides.^{15,16,22}

$$\frac{I_1}{I_2} = C \frac{(3 \cos^2 \gamma - 1)(3 \cos^2 \theta_1 - 1) + 2}{(3 \cos^2 \gamma - 1)(3 \cos^2 \theta_2 - 1) + 2} \quad (1)$$

Here, I_1 and I_2 are the intensity of amide I and amide II bands, C represents the scaling constant ($C = 1.5$, the absorbance ratio of amides I and II for randomly oriented helical structures),²³ γ is the tilt angle of the helix axis from the surface normal and θ is the angle between the transition moment of amide vibration mode and the helix axis. According to the literature, 39° and 75° were used for θ_1 and θ_2 values.²⁴ The value of the tilt angle obtained using IRRAS spectrum was 53° when using a 1 mM solution of peptide **1**. So, in agreement with results reported with other helical peptides,^{15,16,25,26} this value represents an average of all the tilt angles of peptide nanostructures **1** on the surface and demonstrates that they are oriented with the *N*-terminal ligand sticking out, exposed, and not simply absorbed parallel to the gold surface. Similar results for tilt angle were obtained by Williams and Gupta with SAMs formed from poly(Glu) samples²⁷ and by Kimura and co-workers¹⁶ with SAMs formed from Lys/Aib and Ala/Aib polypeptides. Taking into account the significant absorbance of the crown ether amino acid (1516 cm^{-1}) near the amide II region, the peptide tilt angle obtained for SAMs formed with **1** (53°) is a maximum value. Absorbance values of amide II are amplified by the 1516 cm^{-1} absorption of the side



Scheme 2

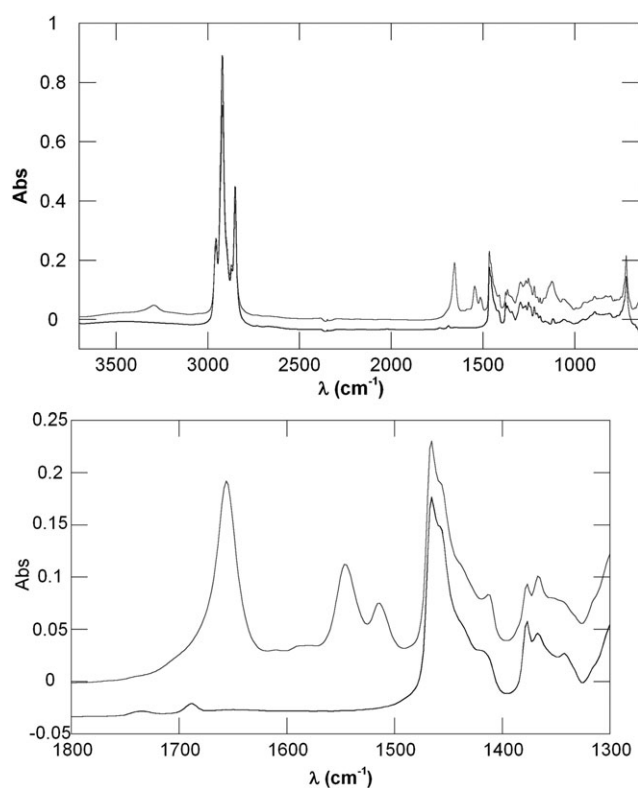


Fig. 3 ATR spectra of gold nanoparticles prepared with pure C_{18} alkane thiol (lower black line) and with a mixture of peptide nanostructure **1** and $C_{18}SH$ (upper grey trace). Top panel: Complete spectra. Bottom panel: Enlargement of the 1300–1800 cm^{-1} region.

chains, which increases the value of tilt angle. In trying to decrease the tilt angle towards more perpendicular nanostructures, we performed the incubation with a less concentrated solution (0.1 mM). However, in this case, a slightly higher value of tilt angle (58°) was observed. Hence, more work is necessary to define the best experimental conditions needed to obtain peptide nanostructures oriented closer to 0° from the surface normal.

To support these results, the PM-IRRAS spectra were recorded from the same monolayer samples. The amide absorption region of the spectrum is shown in Fig. 6. The positive absorption of the amide I band is commonly associated with a tilt angle of between 45 and 90° (see Fig. 6

right).²⁸ Supporting results from IRRAS, spectra obtained with PM-IRRAS from gold surfaces prepared with 0.1 and 1 mM solutions of nanostructure **1** revealed a difference in the amide region. The “shape” of the amide I band gained a slightly negative tendency with increasing concentration. This change in PM-IRRAS spectra can be interpreted by a modification of peptide orientation and suggests an increasing proportion of nanostructures perpendicular to the gold surface. However, disappearance of the amide II band has been attributed to a preponderance of structures parallel to the surface.^{28,29} The solubility of peptide nanostructure **1** in TFE prevents the use of a more concentrated solution.

To confirm the orientation results from IRRAS, we studied the peptide/gold monolayers by AFM (atomic force microscopy). Surface morphology studies revealed the presence of cylindrical clusters of peptides (Fig. 7). The diameters of these clusters vary from 20 to 60 nm. Analysis of AFM images shows, as expected, different structure heights. Interestingly, we observed a lot of cluster summits with heights from 5 to 6 nm, fitting very well with the peptide nanostructure **1** estimated dimension, 5.3 nm (see Fig. 8). The estimation of peptide length was made by molecular modeling³⁰ using Amber94 as forcefield. These results support the hypothesis of a predominance of peptide nanostructures closer to a perpendicular orientation on the gold surface, rather than chemisorbed flat on the surface.

Conclusions

We have described the design, the synthesis, and the characterization of engineered peptide nanostructures bearing a reporter group (biotin) and an anchoring group (lipoamide). This compound was constructed for use as a nanoscale “transducer” in future diagnostic devices for bioanalytical applications at the single molecule level. The results reported illustrate the efficiency of chemisorption of such nanostructures on gold material. We have demonstrated that linking a reporter group and an anchoring site does not affect the α -helical content of the nanostructure framework. Furthermore, when chemisorbed on a gold support, **1** retains a high helical content as proven by IR studies indicating a strong amide I band at 1656 cm^{-1} typical of α -helical structures. Also, results obtained with IRRAS and PM-IRRAS confirmed that in SAMs prepared with a solution of **1** in TFE,

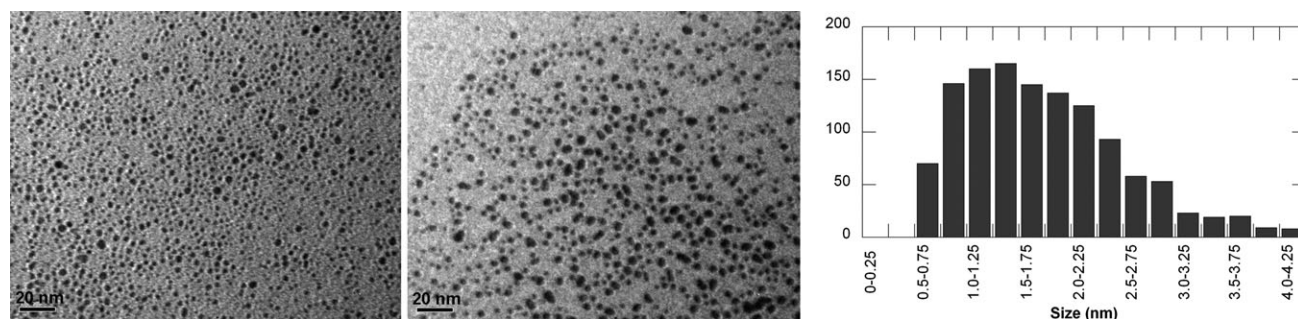


Fig. 4 Left: TEM image of peptide **1**/ $C_{18}SH$ functionalized gold nanoparticles. Middle: TEM image of $C_{18}SH$ functionalized gold nanoparticles. Right: Size distribution histogram for nanoparticles functionalized with **1** and $C_{18}SH$.

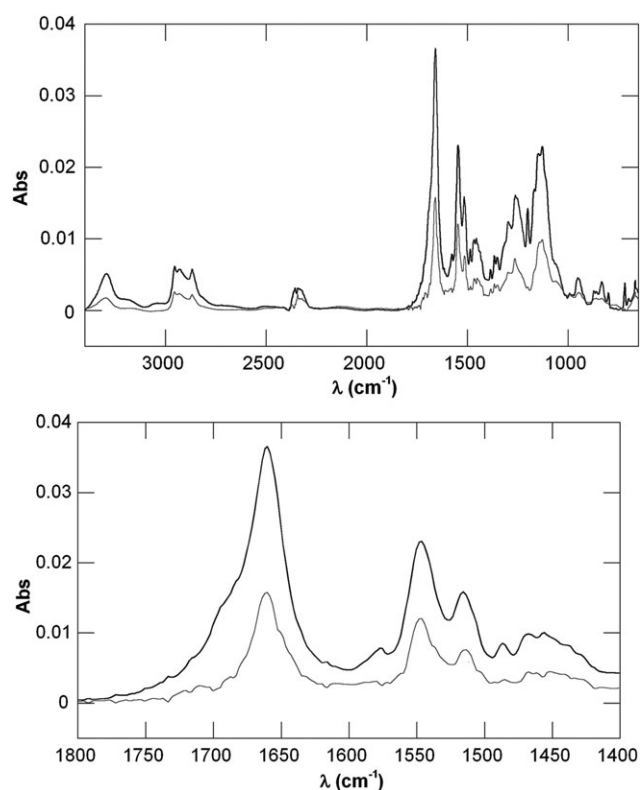


Fig. 5 FT-IRRAS spectrum of peptide nanostructure **1** chemisorbed on a gold surface. Top: Complete spectrum. Bottom: Enlargement of the 1400–1800 cm^{-1} region showing the amide I and II bands. Upper black line: 1 mM solution, and lower grey line: 0.1 mM solution.

the nanostructures are oriented regularly with tilt angles of 53° to 58° on average and are not flat on the gold surface. This conclusion is further supported by AFM studies that demonstrated a monolayer composed of peptide clusters having an average height of 5–6 nm, very close to the calculated length of nanostructure **1**. These results illustrate that **1** and its analogs retain their “functional” conformation and adopt a desired “sticking up” orientation when chemisorbed on gold. These characteristics are necessary for the eventual use of such molecular transducers in future state-of-the-art diagnostic devices. Work is currently in progress to confirm the orientation and organization of **1** using STM,²² and towards the preparation and characterization of mixed SAMs for use in sensitive detection assays.

Experimental

General

Wang resin was purchased from Advanced ChemTech, Louisville, KY, USA. Resins with a substitution level of around 0.7 mmol per gram of benzyl alcohol group were used. Fmoc-protected amino acids were purchased from Matrix Innovation (Quebec City, QC, Canada). All solvents were Reagent, Spectro, or HPLC grade quality purchased commercially and used without any further purification, except for DMF (degassed with N_2), dichloromethane (distilled), and diethyl ether (distilled from sodium and benzophenone). Water used

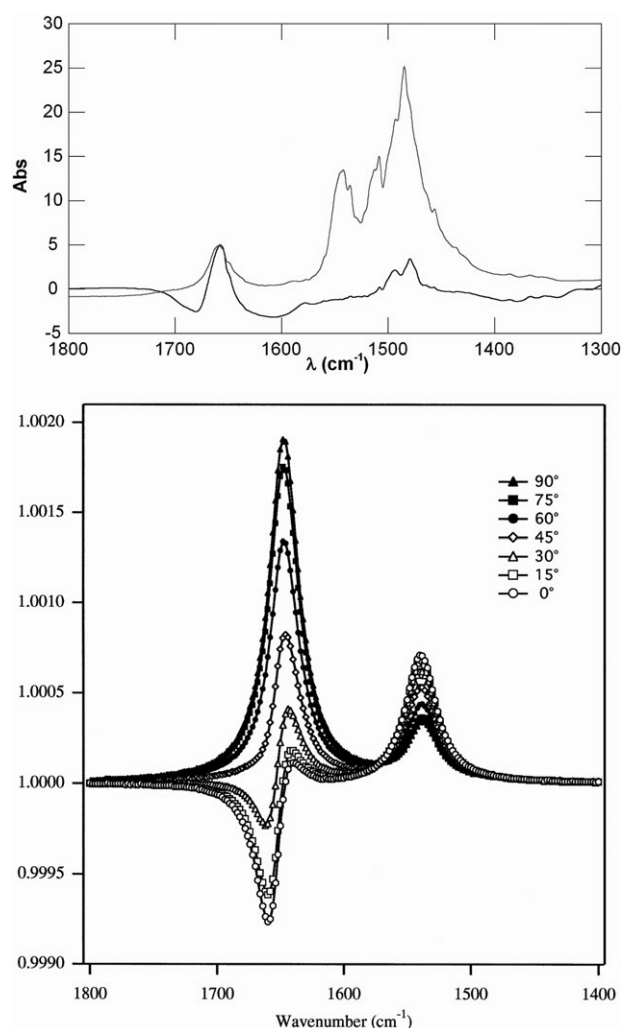


Fig. 6 Top: PM-IRRAS spectra of gold surfaces functionalized with peptide nanostructure **1**; lower black line: 1 mM solution, upper grey line: 0.1 mM solution. Bottom: Calculated PM-IRRAS spectra of the amide I and amide II region of pure α -helices when changing the tilt angle, θ , between the helical axis and the normal to the surface.²⁸

throughout the studies was distilled and deionized using a Barnstead NANOpurII system (Boston, MA, USA) with four purification columns.

Solid phase peptide synthesis was performed manually using solid-phase reaction vessels equipped with a coarse glass frit (ChemGlass, Vineland, NJ, USA). Determination of peptides' purity was performed by reverse phase HPLC with a Vydac C_4 analytical column (Mandel Scientific, ON, Canada). All solvents were degassed and gradients of A (H_2O –0.1% TFA) and B (50% CH_3CN –50% isopropanol–0.1% TFA) were used.

Sonication was done using a Branson water bath model 3510. Mass spectra were obtained from the Mass Spectrometry Laboratory of the Faculty of Medicine of the University of Toronto (Toronto, Canada). Gold-coated chrome slides were purchased from Evaporated Metal Films. Gold substrates were cut from a 3-inch wafer with a diamond-tipped stylus into conveniently sized slides of 2.5×2.5 cm and 1.5×1.5 cm for IRRAS and AFM experiments, respectively. The total thickness of the slides was 1 mm.

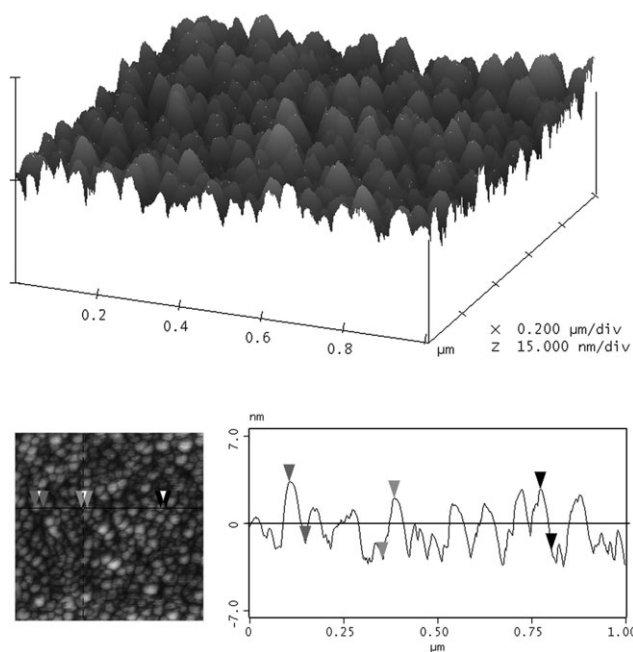


Fig. 7 Above: Surface plot of a gold surface functionalized with peptide nanostructure **1**; Below: Top view of SAM of peptide **1** (left) and a typical section analysis of the peptide clusters showing regular heights between 5 and 6 nm (right).

Synthesis

Crown ether amino acid (CE). The synthesis of the Fmoc-CE amino acid was done using the following protocol. BOC-CE-OH amino acid¹² was dissolved in a minimum of CH_2Cl_2 at 0°C and a solution of 4 M HCl in dioxane (10 equiv.) was added. The mixture was stirred at room temperature until the reaction was completed using TLC for monitoring. The mixture was evaporated and dried under vacuum. The solid obtained was dissolved in a mixture of CH_3CN and H_2O (90 : 10) and cooled at 0°C . DIEA (3 equiv.) and Fmoc-OSu (1.2 equiv.) were added and the mixture was stirred for 2 h at room temperature. The reaction was evaporated and the solid obtained was dissolved in CH_2Cl_2 and washed three times with 1 M HCl and water. The organic phase was dried with MgSO_4 , filtered and evaporated. After several triturations using ether, the desired product was dried under vacuum and obtained in >95% yield as a beige powder. ^1H NMR (CDCl_3) δ : 7.72 (d, 2H, $J = 8$, H ar Fmoc); 7.54 (t, 2H, $J = 7$, H ar Fmoc); 7.36 (t, 2H, $J = 7$, H ar Fmoc); 7.27 (t, 2H, $J = 7$, H ar Fmoc); 6.76–6.73 (m, 2H, H ar CE aa ($\text{H}_5 + \text{H}_6$)); 6.64 (d, 1H, $J = 8$, H ar CE aa (H_2)); 5.37 (d, 1H, $J = 8$, NH); 4.62–4.58 (m, 1H, $\text{CH}\alpha$); 4.41–4.31 (m, 2H, CH_2 Fmoc); 4.17 (t, 1H, CH Fmoc); 4.11–4.09 (m, 2H, $\text{CH}_2\text{-O-Ar}$); 3.86–3.82 (m, 2H, $\text{CH}_2\text{-O-Ar}$); 3.73–3.6 (m, 20H, $\text{O-CH}_2\text{CH}_2\text{-O}$); 3.04 (d, 2H, $J = 5$, $\text{CH}_2\beta$). ESMS m/z 666 (M^+), 683 ($\text{M} + \text{NH}_4^+$).

Peptide synthesis. Typical procedure for peptide synthesis on solid-phase: the amino acid (5 equiv.) was activated with DIC/HOBt during 30 min at 0°C in DMF, and then added to the Wang resin swollen in DMF, followed by addition of

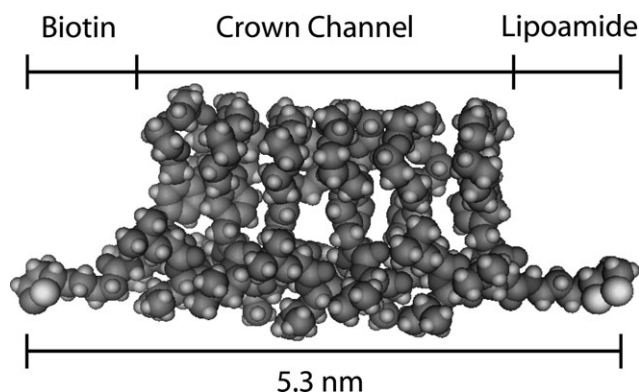


Fig. 8 Length of peptide nanostructure **1** estimated by molecular modeling after minimization.

1.5 equiv. of DIEA. The mixture was shaken mechanically for 2 h at room temperature. The resin was filtered and washed thoroughly with DMF (3×50 mL), MeOH (3×50 mL), DMF (3×50 mL), MeOH (3×50 mL) and then dried *in vacuo*. The completion of coupling reactions was monitored by the ninhydrin test. When necessary, a second coupling was performed under the same condition. The Fmoc group was deprotected by a 15 min treatment with 20% piperidine-DMF.

Biotin was coupled using its *N*-OSu derivatives to the deprotected *N*-terminal.¹⁴ Peptide cleavage was effected using a 95% TFA solution for 1 h. Filtration and evaporation gave the crude free acid peptide. Functionalization of the *C* terminal with lipoamine¹⁸ was performed using EDC coupling agent in DMF for 4 h. The crude peptide **1** was purified and characterized by MS. MS (MALDI): m/z 4686 ($\text{M} + \text{Na}^+$). A purity of >95% was confirmed by RP-HPLC ($R_t = 46$ min).

Gold nanoparticle synthesis. Gold nanoparticles were prepared by adapting a reported protocol.⁷ Hydrogen tetrachloroaurate was dissolved in distilled water (0.30 g in 50 mL of water). Tetraoctylammonium bromide (1.5 equiv.) was dissolved in 50 mL of toluene. This solution was added to the water solution and the mixture was stirred for 15 min, open to air. Thiols (1.1 equiv. relative to gold particles) and peptide were then added and the mixture stirred for another 15 min. Sodium borohydride was dissolved in a minimum amount of water (10 moles relative to gold) and poured in the water/toluene mixture at once. The resulting solution was stirred for 3 h. The toluene layer was separated and transferred into an Erlenmeyer flask, then diluted with ethanol. Samples were then placed in a freezer for a few hours, until the majority of the colloid separated. The solution was then centrifuged at 15000 rpm and the solid was collected by dissolving it in dichloromethane. The solvent was evaporated. Purification was achieved by repeated ethanol precipitation and by centrifugation of the samples.

Transmission electronic microscopy (TEM) images were recorded with a JEOL JEM-1230 at an accelerating voltage of 80 kV. Samples were prepared by allowing a drop of the nanoparticles in solution (CHCl_3) to dry directly on a Formvar/carbon coated nickel microscope grid.

Preparation of SAMs on gold. Gold slides were prepared and cleaned using the following protocol. Gold substrates were immersed in a beaker filled with deionized water and sonicated at room temperature for 1 h. Gold slides were then rinsed extensively with deionized water and TFE, and were immediately used for chemisorption. Chemisorption of the peptide was realized by the direct immersion of the gold substrates freshly washed into solutions (concentrations of 0.1 and 1.0 mM of peptide **1** in TFE) at room temperature. Incubations of 12 to 24 h were achieved before analysis. Following chemisorption, the samples were rinsed several times with TFE to eliminate adventitious contaminants. The samples were then dried under a stream of nitrogen prior to analysis.

Characterization. FT-IRRAS spectra were recorded with a Nicolet OMNIC 3.X infrared spectrophotometer. Spectra were analyzed with the Omnic 3.0 software package (Nicolet, Madison, WI, USA). Grazing angle spectra peptide on gold surface was obtained by using 400 scans with *p*-polarized light at an angle of incidence of 80°.

PM-IRRAS³¹ spectra were collected using a Magna 850 IR spectrophotometer (Nicolet, Madison, WI) with two-channel real-time processing capability. The beam was polarized with a ZnSe linear polarizer (SPECAC, Paris, France) and photoelastically modulated by a ZnSe modulator (Hinds Instruments, Hillsboro, OR), which superimposes a polarization modulation at a fixed frequency (74 kHz). After reflection from the gold surface, the light beam was focused on a photovoltaic Kolmar MCT detector. After electronic filtration and demodulation by a lock-in amplifier (SR830, Stanford Research Systems, Sunnyvale, CA) of the doubly modulated component, signal was processed and Fourier transformed. 128 Scans were collected and recorded with a 4 cm⁻¹ resolution.

AFM images were obtained with Multimode Nanoscope III (Digital Instruments, Santa Barbara, CA) in tapping mode and image analyzed with the Nanoscope Software System. Silicon etched tips (MikroMasch, Wilsonville, OR) were used. The image shown is representative of all images obtained at various positions.

Acknowledgements

This work was supported by the NSERC of Canada, the FQRNT of Quebec, and the Université Laval. J. M. B. is grateful to the CREFSIP for a Postgraduate Scholarship. We are indebted to N. Desgagné and P. Basque for their assistance in performing AFM experiments. We also thank F. Lapointe, T. Lefèvre and M. Pézolet for their help with ATR and IRRAS analyses as well as H. Y. Lelièvre for help with TEM.

References

- 1 J. S. Schultz, *Sci. Am.*, 1991, **265**, 64–69.
- 2 (a) A. Sadana, in *Engineering Biosensors: Kinetics and Design Applications*, Academic Press, San Diego, CA, 2002; (b) P. Fortina, L. J. Kricka, S. Surrey and P. Grodzinski, *Trends Biotechnol.*, 2005, **23**, 168–173; (c) J. Castillo, S. Gaspar, S. Leth, M. Niculescu, A. Mortari, I. Bontidean, V. Soukharev, S. A. Dorneanu, A. D. Ryabov and E. Csoregi, *Sens. Actuators, B*, 2004, **102**, 179–194; (d) W. J. Cooper and M. L. Waters, *Curr. Opin. Chem. Biol.*, 2005, **9**, 627–631; (e) Y. Umezawa and H. Aoki, *Anal. Chem.*, 2004, **76**, 320A–326A.
- 3 N. C. Tansil and Z. Gao, *Nanotoday*, 2006, **1**, 28–37.
- 4 M. Keusgen, *Naturwissenschaften*, 2002, **89**, 433–444.
- 5 R. Shenhar and V. M. Rotello, *Acc. Chem. Res.*, 2003, **36**, 549–561.
- 6 M. C. Daniel and D. Astruc, *Chem. Rev.*, 2004, **104**, 293–346.
- 7 M. Brust, M. Walker, D. Bethell, D. J. Schiffrin and F. Whyman, *J. Chem. Soc., Chem. Commun.*, 1994, 801–802.
- 8 L. Pasquato and P. Pengo, *Spec. Chem. Mag.*, 2003, 38–40.
- 9 C. D. Bain, E. B. Y.-T. Tao, J. Evall, G. M. Whitesides and R. G. Nuzzo, *J. Am. Chem. Soc.*, 1989, **111**, 321–335.
- 10 N. Voyer, M. Arsenault and F. Otis, *Proc. SPIE-Int. Soc. Opt. Eng.*, 2005, **5969**, 125–132.
- 11 N. Voyer, *J. Am. Chem. Soc.*, 1991, **113**, 1818–1821.
- 12 E. Biron, F. Otis, J.-C. Meillon, M. Robitaille, J. Lamothe, P. Van Hove, M.-E. Cormier and N. Voyer, *Bioorg. Med. Chem.*, 2004, **12**, 1279–1290.
- 13 M. J. Swamy and D. Marsh, *FEBS Lett.*, 1993, **324**, 56–58.
- 14 M. Wilchek and E. A. Bayer, *Methods Enzymol.*, 1990, **184**, 123–138.
- 15 X. Wen, R. W. Linton, F. Formaggio, C. Toniolo and E. T. Samulski, *J. Phys. Chem. A*, 2004, **108**, 9673–9681.
- 16 Y. Miura, S. Kimura, Y. Imanishi and J. Umemura, *Langmuir*, 1998, **14**, 6935–6940.
- 17 T. Morita, S. Kimura and S. Kobayashi, *J. Am. Chem. Soc.*, 2000, **122**, 2850–2859.
- 18 R. Barattin and N. Voyer, unpublished work.
- 19 (a) M. J. Hostetler, A. C. Templeton and R. W. Murray, *Langmuir*, 1999, **15**, 3782–3789; (b) A. C. Templeton, M. J. Hostetler, E. K. Warmoth, S. W. Chen, C. M. Hartshorn, V. M. Krishnamurthy, M. D. E. Forbes and R. W. Murray, *J. Am. Chem. Soc.*, 1998, **120**, 4845–4849; (c) P. Ionita, B. C. Gilbert and V. Chechik, *Angew. Chem., Int. Ed.*, 2005, **44**, 3720–3722.
- 20 D. F. Kennedy, M. Crisma, C. Toniolo and D. Chapman, *Biochemistry*, 1991, **30**, 6541–6548.
- 21 W. G. Golden, D. D. Saperstein, M. W. Severson and J. Overend, *J. Phys. Chem.*, 1984, **88**, 574–580.
- 22 K. Kitagawa, T. Morita and S. Kimura, *J. Phys. Chem. B*, 2004, **108**, 15090–15095.
- 23 E. P. Enriquez and E. T. Samulski, *Mater. Res. Soc. Symp. Proc.*, 1992, **225**, 423–434.
- 24 M. Tsuboi, *J. Polym. Sci.*, 1962, **59**, 139–153.
- 25 S. Sek, A. Tolak, A. Misicka, B. Palys and R. Bilewicz, *J. Phys. Chem. B*, 2005, **109**, 18433–18438.
- 26 M. Higuchi, T. Koga, K. Taguchi and T. Kinoshita, *Chem. Commun.*, 2002, 1126–1127.
- 27 A. J. Williams and V. K. Gupta, *J. Phys. Chem. B*, 2001, **105**, 5223–5230.
- 28 I. Cornut, B. Desbat, M. Turlet and J. Dufourcq, *Biophys. J.*, 1996, **70**, 305–312.
- 29 D. Blaudez, J. M. Turlet, J. Dufourcq, D. Bard, T. Buffeteau and B. Desbat, *J. Chem. Soc., Faraday Trans.*, 1996, **92**, 525–530.
- 30 Using software MOE, version 2003.02; Chemical Computing Group, Montréal, Québec, Canada.
- 31 H. Bourque, I. Laurin and M. Pezolet, *Langmuir*, 2001, **17**, 5842–5849.